HHS Public Access

Author manuscript

Nat Med. Author manuscript; available in PMC 2012 July 01.

Published in final edited form as:

Nat Med. ; 18(1): 172–177. doi:10.1038/nm.2590.

In Vivo Imaging of Ligand Receptor Binding with *Gaussia* Luciferase Complementation

Kathryn E. Luker[1], **Laura Anne Mihalko**[1,#], **Bradley T. Schmidt**[1,#], **Sarah A. Lewin**[1], **Paramita Ray**[1], **Dmitry Shcherbo**[2], **Dmitriy M. Chudakov**[2,3], and **Gary D. Luker**[1,4,5]

[1]Center for Molecular Imaging, Department of Radiology, University of Michigan Medical School, Moscow, Russia

[2]Shemyakin and Ovchinnikov Institute of Bioorganic Chemistry RAS, Moscow, Russia

[3]Nizhny Novgorod State Medical Academy, Nizhny Novgorod, Russia

[4]Department of Microbiology and Immunology, University of Michigan Medical School, Ann Arbor, MI, USA

Abstract

Studies of ligand-receptor binding and development of receptor antagonists would benefit greatly from imaging techniques that translate directly from cell-based assays to living animals. We used *Gaussia* luciferase protein fragment complementation to quantify binding of chemokine CXCL12 to receptors CXCR4 and CXCR7. Small molecule inhibitors of CXCR4 or CXCR7 specifically blocked CXCL12 binding in cell-based assays, and these studies revealed differences in kinetics for inhibiting chemokine binding to each receptor. Bioluminescence imaging showed CXCL12-CXCR7 binding in primary and metastatic tumors in a mouse model of breast cancer. We also used this imaging technique to quantify drug-mediated inhibition of CXCL12-CXCR4 binding in living mice. We expect this imaging technology to advance research in areas including ligand-receptor interactions and development of new therapeutic agents in cell-based assays and small animals.

Keywords

breast cancer; chemokines; chemokine receptors; bioluminescence imaging; luciferase; protein fragment complementation

[5]Correspondence: Gary D. Luker, Center for Molecular Imaging, University of Michigan Medical School, 109 Zina Pitcher Place, A526 BSRB, Ann Arbor, MI, USA 48109-2200. gluker@umich.edu. Phone: 734-763-5476. Fax: 734-763-5447..

[#]these authors contributed equally to the work.

Author Contributions K.L., L.M., B.S., S.L., P.R., and G.L. performed cell culture and animal experiments and analyzed data. K.L., D.S., D.C., and G.L. provided new reagents. K.L., B.S., D.C., and G.L. prepared the manuscript. K.L. and G.L. supervised the project.

Conflict of Interest Statement The authors declare no competing financial interests.

Introduction

Ligand-receptor binding initiates signal transduction, and therapeutic agents targeting cell surface receptors predominantly block ligand binding. The central importance of ligand-receptor binding in normal signaling, disease, and drug development emphasizes the need for improved technologies to analyze ligand-receptor complexes in intact cells and living animals. Ligand-receptor binding currently is quantified with fluorescent or radioactive ligands. Such labels produce signal independent of receptor binding, generating background that limits detection of ligand-receptor complexes. Furthermore, a labeled ligand detects all accessible receptors rather than the subset of receptors actively signaling. Developing an imaging assay to quantify ligand-receptor complexes under physiologic conditions will substantially advance studies of multiple diseases and accelerate drug development.

Receptors CXCR4 and CXCR7, both of which bind chemokine CXCL12, are promising therapeutic targets for cancer and other diseases. CXCR4 promotes tumor growth and metastasis in more than 20 cancers, and recent pre-clinical studies show similar effects for CXCR7M[1,2,3]. Malignant cells in breast, ovarian, and other cancers secrete CXCL12 and/or express CXCR4 and/or CXCR7. CXCL11, the second ligand for CXCR7, also is present in tumorsM[4–6]. Agents blocking chemokine binding to these receptors are being developed for cancer therapy, highlighting the need for improved methods to image ligand-receptor complexes *in vivo*.

We used *Gaussia* luciferase (GLuc) complementation, a fully reversible system, to image chemokine-receptor binding[7]. GLuc fragments are inactive, so there is minimal background bioluminescence. Since GLuc does not require ATP, this system detects ligand-receptor complexes intracellularly and in the extracellular space. GLuc also is smaller than other luciferases and fluorescent proteins, minimizing potential steric effects of fusing enzyme fragments to proteins of interest. Using GLuc complementation, we quantified chemokine binding to CXCR4 and CXCR7 and inhibition with small molecules in cell-based assays and living mice, providing a novel method to link *in vitro* and *in vivo* testing of therapeutic agents.

Results

GLuc complementation for ligand-receptor binding

To identify optimal orientations of fusion proteins, we fused N- or C-terminal fragments of GLuc (NGLuc and CGLuc) to the C-terminus of CXCL12 and N-terminus of CXCR7 or CXCR4. These fusions position NGLuc and CGLuc in the extracellular space (Fig. 1a). As controls for non-specific association of GLuc fragments, we also generated secreted, unfused NGLuc and CGLuc. We transfected cells with a single reporter, secreted NGLuc or CGLuc controls, or vector and seeded equal numbers of matched pairs of cells in 96 well plates. Following overnight co-culture, the combination of cells expressing CXCL12-CGLuc and NGLuc-CXCR7 generated bioluminescence >10-fold above background, which was greater than all other combinations (Fig 1b). Similarly, complementation between CXCL12-CGLuc and NGLuc-CXCR4 was higher than other pairs of co-cultured cells (Fig 1c). Flow cytometry showed comparable expression of matched pairs of receptor fusion proteins (Fig

S1). We selected CXCL12-CGLuc and NGLuc-CXCR7 or NGLuc-CXCR4 fusions for subsequent studies.

To quantify bioluminescence following a pulse of CXCL12, we incubated cells expressing NGLuc-CXCR7, NGLuc-CXCR4, or control protein CXCR7-GFP for 15 minutes with CXCL12-CGLuc or CGLuc. Complementation between CXCL12-CGLuc and NGLuc-CXCR4 or NGLuc-CXCR7 produced more light than CGLuc, the latter of which was comparable to CXCR7-GFP (Fig 1d). CXCL12-CGLuc binding to NGLuc-CXCR7 produced more bioluminescence than NGLuc-CXCR4, likely due to greater binding affinity, relatively higher levels of cell surface CXCR7 that do not desensitize upon ligand binding, and prolonged intracellular association of CXCL12 with CXCR7 [8,9,10,11].

To test complementation between CXCR7 and CXCL11 and identify conditions that maximize bioluminescence, we co-cultured cells expressing NGLuc-CXCR7 with various ratios of cells secreting CXCL11-CGLuc or CXCL12-CGLuc. CXCL12-CGLuc binding to NGLuc-CXCR7 produced ≈20-fold more light than CXCL11-CGLuc, corresponding with ≈20–50-fold greater binding affinity of CXCR7 for CXCL12[8,9]. Peak bioluminescence occurred at 1:1 ratios of chemokine-secreting and NGLuc-CXCR7 cells (Fig S2a, b), so we used this ratio for subsequent experiments. These data also show the assay is not restricted to CXCL12.

Inhibiting chemokine-receptor binding in cell-based assays

We generated MDA-MB-231 breast cancer cells secreting CXCL12-CGLuc or CGLuc or expressing NGLuc-CXCR7 or NGLuc-CXCR4. 231-CXCL12-CGLuc and CGLuc cells expressed equivalent levels of CGLuc by QRT-PCR (data not shown). 231-CXCL12-CGLuc cells secreted ≈ 1 ng/cell/hour of chemokine, which is sufficient to activate CXCR4[12]. 231-NGLuc-CXCR7 cells had slightly higher surface expression and binding sites for CXCL12 than 231-NGLuc-CXCR4 cells (Fig S3a, b; S4a, b). NGLuc-CXCR7 retained the chemokine scavenging function of CXCR7 (Fig S5)[10].

We co-cultured 231-CXCL12-CGLuc or 231-CGLuc cells with 231-NGLuc-CXCR7 cells for 16 hours with CXCR7 inhibitors (CCX733, CCX771), an inactive analog (CCX704), or CXCR4 inhibitor (AMD3100). CXCR7 inhibitors reduced complementation between CXCL12-CGLuc and NGLuc-CXCR7 to levels from the control pair of CGLuc and NGLuc-CXCR7 (Fig 2a). Neither CCX704 nor AMD3100 had any effect. Both CXCR7 inhibitors also reduced bioluminescence from CXCL11-CGLuc binding to NGLuc-CXCR7 without affecting minimal signal from CXCL11-CGLuc and NGLuc-CXCR4 (Fig S6). CCX733 and CCX771 produced dose-dependent inhibition of CXCL12-CGLuc and NGLuc-CXCR7 complementation, while CCX704 was ineffective (Fig 2b). CCX733 also was more effective than CCX771 at blocking CXCL12 binding to cell surface NGLuc-CXCR7 (Fig S7).

CXCR7 and chemokine ligands co-localize within cells, suggesting that ligand-receptor complexes remain intact for extended time[10,11]. To investigate kinetics of inhibiting CXCL12 binding to CXCR7, we incubated co-cultures of 231-CXCL12-CGLuc and 231-NGLuc-CXCR7 cells with increasing concentrations of CCX733 for 6 or 24 hours (Fig 2c). Treatment with 1 μM CCX733 for 24 hours reduced bioluminescence to levels produced by

231-CGLuc and 231-NGLuc-CXCR7, while less inhibition occurred after 6 hours. Inhibition of CXCL12-CGLuc/NGLuc-CXCR7 complementation with 300 nM CCX733 required 4 hours, and bioluminescence decreased further at 6 hours (Fig 2d). AMD3100 had no effect. These results suggest that bioluminescence decreases because CXCR7 inhibitors block new CXCL12-CXCR7 complexes in the extracellular space, while internalized complexes remain intact until degradation of chemokine in lysosomes[11].

Bioluminescence from co-cultures of 231-CXCL12-CGLuc and 231-NGLuc-CXCR4 cells decreased to levels comparable to CGLuc with NGLuc-CXCR4 following overnight incubation with 1 μM AMD3100 (Fig 3a). CXCR7 inhibitors did not alter complementation between CXCL12-CGLuc and NGLuc-CXCR4, and no compound changed bioluminescence from 231-CGLuc and 231-NGLuc-CXCR4 cells. AMD3100 produced dose-dependent inhibition of CXCL12-CGLuc/NGLuc-CXCR4 complementation down to levels produced by CGLuc and NGLuc-CXCR4 (Fig 3b). CXCL12-CGLuc/NGLuc-CXCR4 complementation was unaffected by CCX733 or CCX771, and no compound altered control signals from CGLuc and NGLuc-CXCR4.

To analyze kinetics of inhibition, we treated co-cultures of 231-CXCL12-CGLuc and 231-NGLuc-CXCR4 cells with 300 nM AMD3100 or CCX733. Bioluminescence decreased after 1 hour with AMD3100, and maximum inhibition occurred by 4 hours (Fig 3c). CCX733 had no effect. These data revealed that inhibition of CXCL12-CGLuc binding to NGLuc-CXCR4 occurs more rapidly than NGLuc-CXCR7.

Imaging CXCL12-CXCR7 binding *in vivo*

We orthotopically implanted 231-NGLuc-CXCR7 cells with 231-CXCL12-CGLuc or 231-CGLuc cells in mammary fat pads of mice, reproducing expression of CXCR7 or secretion of CXCL12 in human breast tumors[2,13]. 231-NGLuc-CXCR7 cells also expressed firefly luciferase (FLuc) and green fluorescent protein (GFP) for imaging *in vivo* and *ex vivo*, respectively. 231-CXCL12-CGLuc/231-NGLuc-CXCR7 tumors had robust GLuc bioluminescence, while 231-CGLuc/231-NGLuc-CXCR7 tumors were undetectable (Fig S8a, b). By comparison, FLuc imaging 4 days earlier showed comparable numbers of 231-NGLuc-CXCR7 cells in both groups. Consistent with cell-based assays, CXCL12-CGLuc and NGLuc-CXCR7 tumors also produced more GLuc bioluminescence than tumors with CXCL12-CGLuc and NGLuc-CXCR4 (Fig S9). These data establish that GLuc complementation imaging detects quantitative differences in ligand-receptor binding *in vivo*.

To image 231-CXCL12-CGLuc and NGLuc-CXCR7 cells independently, we transduced 231-CXCL12-CGLuc cells with far red fluorescent protein eqFP650[14]. Fluorescence from eqFP650 in 231-CXCL12-CGLuc cells and luminescence from FLuc in 231-NGLuc-CXCR7 cells co-localized in primary tumors. Since light from FLuc in primary tumors shone over the entire mouse during longer imaging times, we removed primary tumors and analyzed metastases in internal sites. eqFP650 fluorescence and FLuc bioluminescence co-localized in multiple metastases, which was confirmed by fluorescence microscopy (Fig 4a, b). Flow cytometry showed ≈2:1 ratio of 231-NGLuc-CXCR7 to 231-CXCL12-CG cells in both dissociated primary tumors and metastases.

Co-localization of 231-CXCL12-CGLuc and 231-NGLuc-CXCR7 cells suggested that intercellular chemokine-receptor binding occurs in metastases. We identified metastases with both eqFP650 fluorescence and GLuc bioluminescence, demonstrating CXCL12-CXCR7 binding in sites containing both 231-CXCL12-CGLuc and 231-NGLuc-CXCR7 cells (Fig 4c). We verified co-localization of fluorescence and GLuc complementation from CXCL12-CGLuc binding to NGLuc-CXCR7 in some metastases (Fig 4d, Fig S10). While the maximum distance for intercellular CXCL12-CXCR7 binding has not been determined *in vivo*, CXCR7 cells do not generate a chemotactic gradient when separated by >400 μm from CXCL12-secreting cells *in vitro*[12]. Diffusion of CXCL12 is restricted by proteoglycans, so intercellular ligand-receptor binding likely occurs over much smaller distances in tumors[15]. These data demonstrate that 231-CXCL12-CGLuc and 231-NGLuc-CXCR7 cells may metastasize to the same sites and establish intercellular ligand-receptor binding.

We attempted to inhibit CXCL12-CGLuc and NGLuc-CXCR7 complementation in mice with CCX771. We were unable to significantly reduce complementation *in vivo*, likely because blocking this interaction requires prolonged exposure to relatively high levels of compound.

Imaging inhibition of CXCL12-CXCR4 binding *in vivo*

We implanted orthotopic tumors with 231-CXCL12-CGLuc and 231-NGLuc-CXCR4 cells. 231-CXCL12-CGLuc cells co-express eqFP650, and 231-NGLuc-CXCR4 cells express firefly luciferase and GFP. These reporters allow independent imaging of both cell populations. After obtaining baseline imaging data, we implanted mice with subcutaneous osmotic infusion pumps delivering either AMD3100 or PBS. Pumps delivered 600 μg of AMD3100 per day, producing serum levels of ≈ 1.25 μM[16]. GLuc complementation decreased by ≈85% after 5 days of treatment with AMD3100, which was comparable to ≈80% inhibition of CXCL12-GLuc binding to intact 231-NGLuc-CXCR4 cells by 1.25 μM AMD3100 *in vitro* (Fig 5a, b). Treatment with AMD3100 reduced bioluminescence from CXCL12-CGLuc and NGLuc-CXCR4 to levels comparable to control 231-CGLuc/231-NGLuc-CXCR4 tumors (Fig S11). GLuc bioluminescence increased by ≈ 50% in mice treated with PBS. After removing infusion pumps with AMD3100, bioluminescence from CXCL12-CXCR4 binding increased within 2 days to levels comparable to mice treated with PBS.

AMD3100 limited growth of 231 cells in primary tumors as quantified by decreased eqFP650 fluorescence from 231-CXCL12-CGLuc cells and a trend toward reduced FLuc activity from 231-NGLuc-CXCR4 cells (Fig 5c, d). Loss of GLuc signal was due primarily to inhibition of CXCL12 binding to CXCR4, since reductions in GLuc bioluminescence greatly exceeded effects of AMD3100 on tumor burden. Mice treated with AMD3100 had fewer metastases than PBS control (≈30% versus 70%, respectively, by FLuc imaging) (Fig 5a). Multiple metastases from 231-CXCL12-CGLuc and 231-NGLuc-CXCR4 cells also were detected by GLuc bioluminescence (Fig S12). These data establish that GLuc complementation can quantify pharmacodynamics of therapy *in vivo*.

Discussion

We developed a GLuc complementation assay to image ligand-receptor complexes under physiologic conditions in cell-based assays and living mice. The same imaging reporters are used for cell culture and animal studies, enabling direct comparisons of ligand binding and targeting of potential therapeutic agents *in vitro* and *in vivo*. GLuc bioluminescence is proportional to numbers of ligand-receptor complexes, providing a quantitative assay to establish targeting of therapeutic agents. Since many pre-clinical drug development studies are designed to achieve defined levels of receptor inhibition at a target site, GLuc complementation provides essential information about receptor coverage in living animals[17,18]. Combining GLuc complementation with additional imaging reporters allows real-time analysis of receptor targeting and resultant effects on tumor growth and metastasis.

While we focused on chemokines and chemokine receptors, this imaging system is directly applicable to any ligand-receptor pair with a peptide ligand that can be fused genetically to a fragment of GLuc. Recombinant GLuc has been purified and fused to other molecules[19,20], so it should be feasible to chemically link a fragment of GLuc to non-peptide ligands. This approach would further extend applications of the technology for cell-based assays and animal imaging. *In vivo* imaging of GLuc complementation in internal organs currently is limited by peak emission at 480 nm, which has limited penetration through tissues. Developing red-shifted mutants of GLuc, as has been accomplished for other luciferases, will improve detection of ligand-receptor complexes and drug targeting in intact mice[21]. We expect this imaging system will have widespread impact in areas including intercellular signaling in tumors and development of therapeutic agents targeting ligand-receptor binding.

Supplementary Material

Refer to Web version on PubMed Central for supplementary material.

Acknowledgments

Research was supported by NIH grants R01 CA136553, R01 CA136829, R01 CA142750, P50 CA93990 (GDL), Measures to Attract Leading Scientists to Russian Educational Institutions program, and Molecular and Cell Biology program RAS (DMC). Research also was supported by NIH grant 1S10RR28819-1. We thank ChemoCentryx for mAb 11G8 and small molecule inhibitors of CXCR7. We acknowledge support from NIH grant U24 CA083099 for the Michigan Small Animal Imaging Resource. We thank Juan Jaen, Mark Penfold, and Dan Dairaghi for helpful discussions.

References

1. Muller A, et al. Involvement of chemokine receptors in breast cancer metastasis. Nature. 2001; 410:50–56. [PubMed: 11242036]
2. Miao Z, et al. CXCR7 (RDC1) promotes breast and lung tumor growth in vivo and is expressed on tumor-associated vasculature. Proc Natl Acad Sci U S A. 2007; 104:15735–15740. [PubMed: 17898181]
3. Wang J, et al. The role of CXCR7/RDC1 as a chemokine receptor for CXCL12/SDF-1 in prostate cancer. J Biol Chem. 2008; 283:4283–4294. [PubMed: 18057003]
4. Hall J, Korach K. Stromal cell-derived factor 1, a novel target of estrogen receptor action, mediates the mitogenic effects of estradiol in ovarian and breast cancer cells. Mol Endocrinol. 2003; 17:792–803. [PubMed: 12586845]

5. Furuya M, et al. Up-regulation of CXC chemokines and their receptors: implications for proinflammatory microenvironments of ovarian carcinomas and endometriosis. Hum Pathol. 2007; 37:1676–1687. [PubMed: 17707463]
6. Shin S, Nam J, Lim Y, Lee Y. TNFα-exposed bone marrow-derived mesenchymal stem cells promote locomotion of MDA-MB-231 breast cancer cells through transcriptional activation of CXCR3 ligand chemokines. J Biol Chem. 2010; 285:30731–30740. [PubMed: 20650898]
7. Remy I, Michnick S. A highly sensitive protein-protein interaction assay based on Gaussia luciferase. Nat Methods. 2006; 3:977–979. [PubMed: 17099704]
8. Balabanian K, et al. The chemokine SDF-1/CXCL12 binds to and signals through the orphan receptor RDC1 in T lymphocytes. J Biol Chem. 2005; 280:35760–35766. [PubMed: 16107333]
9. Burns J, et al. A novel chemokine receptor for SDF-1 and I-TAC involved in cell survival, cell adhesion, and tumor development. J Exp Med. 2006; 203:2201–2213. [PubMed: 16940167]
10. Boldajipour B, et al. Control of chemokine-guided cell migration by ligand sequestration. Cell. 2008; 132:463–473. [PubMed: 18267076]
11. Luker K, Steele J, Mihalko L, Luker G. Constitutive and chemokine-dependent internalization and recycling of CXCR7 in breast cancer cells to degrade chemokine ligands. Oncogene. 2010; 29:4599–4610. [PubMed: 20531309]
12. Torisawa Y, et al. Microfluidic platform for chemotaxis in gradients formed by CXCL12 source-sink cells. Integr Biol (Camb). 2010; 2:680–686. [PubMed: 20871938]
13. Mirisola V, et al. CXCL12/SDF1 expression by breast cancers is an independent prognostic marker of disease-free and overall survival. Eur J Cancer. 2009; 45:2579–2567. [PubMed: 19646861]
14. Shcherbo D, et al. Near infrared fluorescent proteins. Nat Methods. 2010; 7:827–829. [PubMed: 20818379]
15. McCandless E, et al. Pathological expression of CXCL12 at the blood-brain barrier correlates with severity of multiple sclerosis. Am J Pathol. 2008; 172:799–808. [PubMed: 18276777]
16. Datema R, et al. Antiviral efficacy in vivo of the anti-human immunodeficiency virus bicyclam SDZ SID 791 (JM 3100), an inhibitor of infectious cell entry. Antimicrob Agents Chemother. 1996; 40:750–754. [PubMed: 8851605]
17. Woska JJ, et al. Small molecule LFA-1 antagonists compete with an anti-LFA-1 monoclonal antibody for binding to the CD11a I domain: development of a flow-cytometry-based receptor occupancy assay. J Immunol Methods. 2003; 277:101–115. [PubMed: 12799043]
18. Lin L, et al. Discovery of N-{N-[(3-cyanophenyl)sulfonyl]-4(R)-cyclobutylamino-(L)-prolyl}-4-[(3',5'-dichloroisonicotinoyl) amino]-(L)-phenylalanine (MK-0668), an extremely potent and orally active antagonist of very late antigen-4. J Med Chem. 2009; 52:3449–3452. [PubMed: 19441819]
19. Venisnik K, Olafsen T, Gambhir S, Wu A. Fusion of Gaussia luciferase to an engineered anti-carcinoembryonic antigen (CEA) antibody for in vivo optical imaging. Mol Imaging Biol. 2007; 9:267–277. [PubMed: 17577599]
20. Patel K, et al. Cell-free production of Gaussia princeps luciferase--antibody fragment bioconjugates for ex vivo detection of tumor cells. Biochem Biophys Res Commun. 2009; 390:971–976. [PubMed: 19852937]
21. Loening A, Wu A, Gambhir S. Red-shifted Renilla reniformis luciferase variants for imaging in living subjects. Nat Methods. 2007; 4:641–643. [PubMed: 17618292]
22. Lois C, Hong E, Pease S, Brown E, Baltimore D. Germline transmission and tissue-specific expression of transgenes delivered by lentiviral vectors. Science. 2002; 295:868–872. [PubMed: 11786607]
23. Luker K, Gupta M, Luker G. Bioluminescent CXCL12 fusion protein for cellular studies of CXCR4 and CXCR7. Biotechniques. 2009; 47:625–632. [PubMed: 19594447]
24. Smith M, et al. CXCR4 regulates growth of both primary and metastatic breast cancer. Cancer Res. 2004; 64:8604–8612. [PubMed: 15574767]
25. Luker K, Gupta M, Steele J, Foerster B, Luker G. Imaging Ligand-dependent Activation of CXCR7. Neoplasia. 2009; 11:1022–1035. [PubMed: 19794961]

26. Tannous B, Kim D, Fernandez J, Weissleder R, Breakefield X. Codon-optimized Gaussia luciferase cDNA for mammalian gene expression in culture and in vivo. Mol Ther. 2005; 11:435–443. [PubMed: 15727940]

27. Luker G, et al. Noninvasive bioluminescence imaging of herpes simplex virus type 1 infection and therapy in living mice. J Virol. 2002; 76:12149–12161. [PubMed: 12414955]

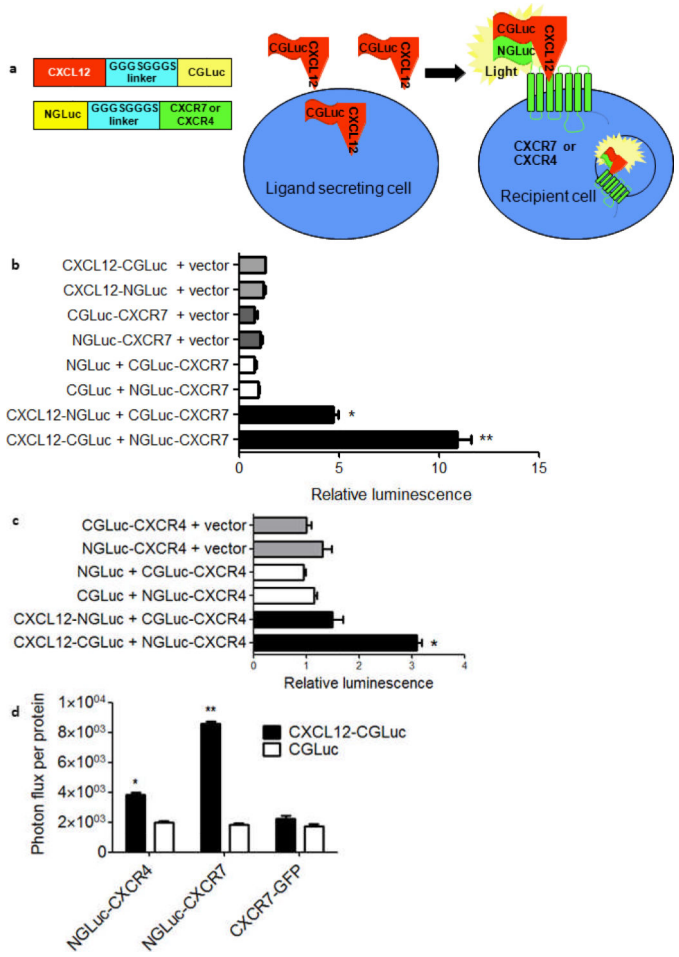

Figure 1. Development of *Gaussia* luciferase (GLuc) complementation for CXCL12 binding to CXCR4 or CXCR7

(a) Schematic diagram of GLuc complementation constructs for imaging ligand-receptor binding both extracellularly and intracellularly. Binding of CXCL12-CGLuc to NGLuc-CXCR4 or NGLuc-CXCR7 reconstitutes GLuc, producing light as a quantitative measure of ligand-receptor binding. **(b, c)** Quantification of GLuc bioluminescence for various orientations and combinations of complementation reporters for CXCR7 (**b**) or CXCR4 (**c**). Data were normalized to bioluminescence from untransfected cells and presented as mean values + SEM for relative luminescence. Note different scales for relative luminescence values for CXCR7 and CXCR4 complementation. **(d)** Quantified data for GLuc bioluminescence after 15 minutes of incubation with CXCL12-CGLuc or unfused, secreted CGLuc. We normalized photon flux data to total protein per well and expressed these results as mean values + SEM. *, $P<0.05$; **, $P<0.01$.

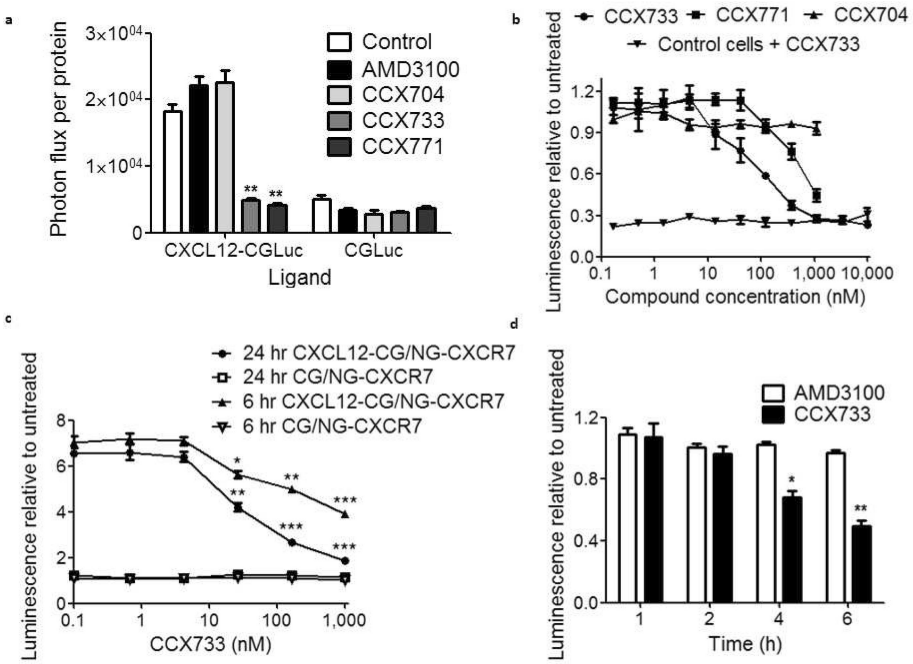

Figure 2. Small molecule inhibitors block GLuc complementation between CXCL12 and CXCR7

(a) Quantified GLuc activity from co-cultures of 231-NGLuc-CXCR7 cells with either 231-CXCL12-CGLuc or 231-CGLuc cells in the presence of 1 μM CXCR7 inhibitors (CCX733, CCX771), inactive CXCR7 compound (CCX704), CXCR4 inhibitor (AMD3100), or vehicle. We normalized bioluminescence to total protein in each well and graphed mean values + SEM. **(b)** GLuc bioluminescence from co-cultures of 231-CXCL12-CGLuc and 231-NGLuc-CXCR7 cells treated overnight with increasing concentrations of CCX733, CCX771, or negative control compound CCX704. Graph also shows bioluminescence from control cells (231-CGLuc and 231-NGLuc-CXCR7) treated with various concentrations of CCX733. We graphed mean values ± SEM for bioluminescence relative to values for untreated cells. **(c)** Quantified GLuc activity from pairs of co-cultured cells (231-CXCL12-CGLuc/231-NGLuc-CXCR7 or control pair 231-CGLuc/231-NGLuc-CXCR7) after incubation for 6 or 24 hours with increasing concentrations of CCX733. Graph shows mean values ± SEM relative to untreated cells. **(d)** Bioluminescence from co-cultures of 231-CXCL12-CGLuc and 231-NGLuc-CXCR7 cells treated for various periods of time with 300 nM CCX733 or AMD3100. Graphs show mean values + SEM for bioluminescence relative to cells treated with vehicle alone. *, $P<0.05$; **, $P<0.01$; ***, $P<0.005$.

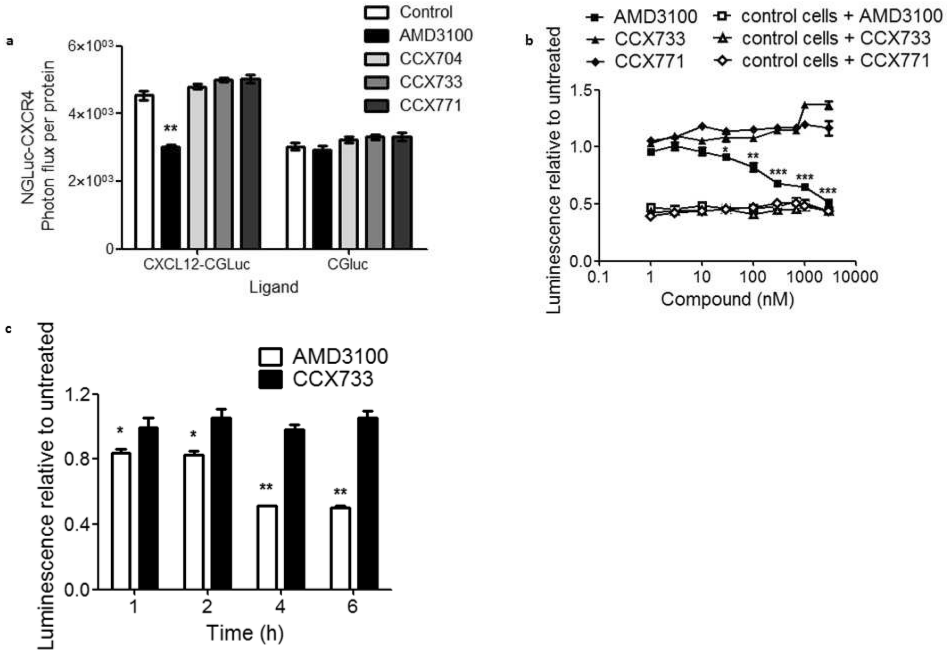

Figure 3. Specific inhibition of CXCL12-CXCR4 complementation in cell-based assays

(a) Quantified GLuc activity from co-cultures of 231-NGLuc-CXCR4 cells with 231-CXCL12-CGLuc or 231-CGLuc cells after overnight incubation with 1 μM AMD3100, CCX704, CCX733, CCX771, or vehicle control. Bioluminescence was normalized to total protein in each well and graphed as mean values + SEM. **(b)** GLuc bioluminescence from cultures of 231-CXCL12-CGLuc and 231-NGLuc-CXCR4 cells or control 231-CGLuc and 231-NGLuc-CXCR4 cells treated with increasing concentrations of AMD3100, CCX733, or CCX771 for 4 hours. Data were presented as GLuc bioluminescence ± SEM relative to cells treated with vehicle control. (**c**) Bioluminescence from co-cultures of 231-CXCL12-CGLuc and 231-NGLuc-CXCR4 cells incubated with 300 nM AMD3100 or CCX733 for various periods of time. Data for GLuc activity were graphed as mean values + SEM for bioluminescence relative to cells treated with vehicle alone. *, $P<0.05$; **, $P<0.01$, ***, $P<0.005$.

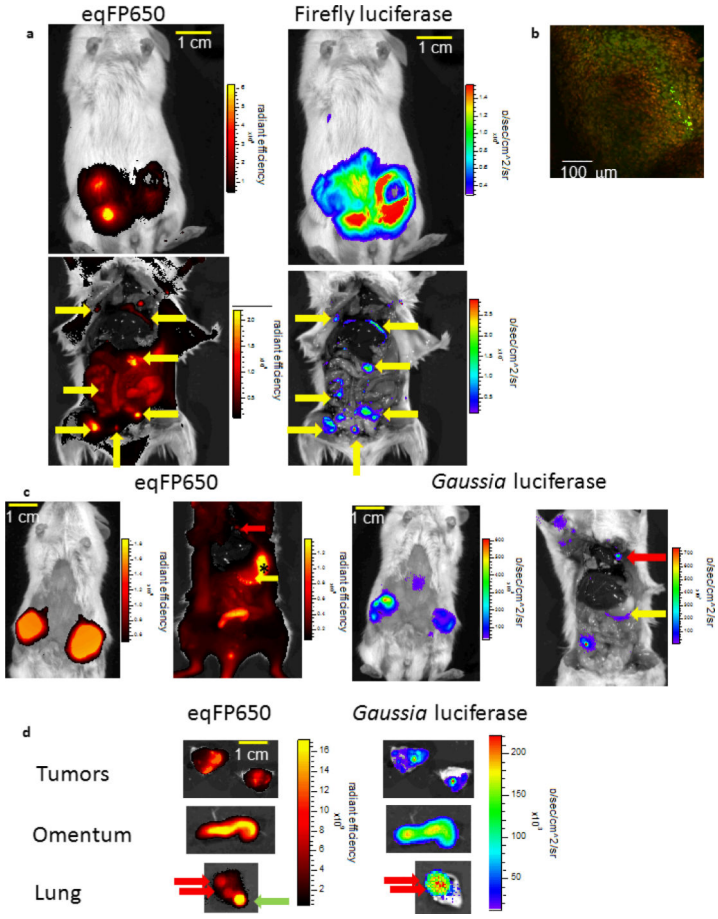

Figure 4. Imaging CXCL12-CXCR7 binding in primary and metastatic breast tumors

(a) Representative fluorescence and bioluminescence images of eqFP650 and FLuc in 231-CXCL12-CGLuc and 231-NGLuc-CXCR7 cells, respectively, in orthotopic breast tumor xenografts. After imaging intact mice, primary tumors were removed and internal organs were exposed to identify metastases. Yellow arrows denote metastases with co-localized 231-CXCL12-CGLuc (eqFP650 fluorescence) and 231-NGLuc-CXCR7 cells (FLuc bioluminescence). Pseudocolor scales depict ranges of values displayed for radiant efficiency and photon flux. Scale bar on image shows 1 cm. **(b)** *Ex vivo* microscopy of a lymph node from the mouse in panel A showing fluorescence from eqFP650 and GFP in 231-CXCL12-GLuc and 231-NGLuc-CXCR7 cells, respectively. Scale bar shows 100 μm. **(c)** Representative eqFP650 fluorescence and GLuc complementation images of intact mice and exposed internal organs of mice with orthotopic tumor xenografts of 231-CXCL12-CGLuc and 231-NGLuc-CXCR7 cells. Arrows show metastases with co-localized eqFP6560 fluorescence (231-CXCL12-CGLuc cells) and GLuc bioluminescence in lung (red arrow) and omentum (yellow arrow). Asterisk denotes fluorescence from retained food in the stomach. **(d)** eqFP650 fluorescence and GLuc bioluminescence images of excised primary tumors and metastatic foci in omentum and lung from the mouse shown in B. Red arrows show lung metastases with co-localized eqFP650 fluorescence and GLuc bioluminescence, respectively. Green arrow shows eqFP650 fluorescence from a metastasis with only 231-CXCL12-CGLuc cells. Scale bar depicts 1 cm.

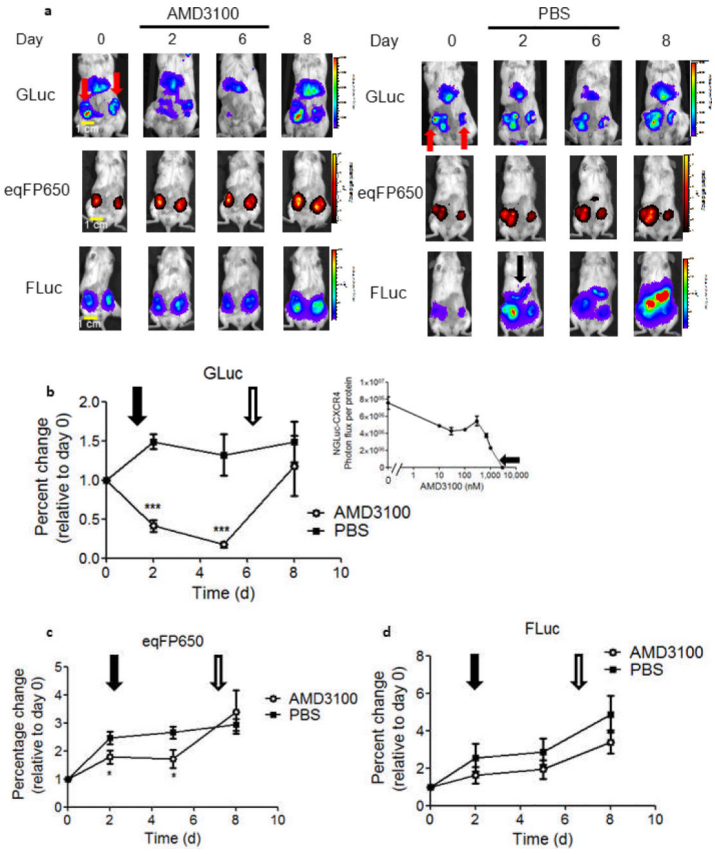

Figure 5. ***In vivo*** **imaging of CXCL12-CXCR4 binding and inhibition**

(**a**) Representative GLuc, eqFP650, and firefly luciferase (FLuc) images of mice prior to treatment (day 0), during treatment with AMD3100 or PBS vehicle control (days 2, 5), and following treatment (day 8). Pseudocolor scale bars denote range of photon flux or radiant efficiency values displayed for each mouse. Scale bar on image is 1 cm. Red arrows show GLuc complementation signal in primary breast tumors. Black arrow denotes FLuc bioluminescence in a metastasis to the omentum. **(b–d)** Quantified data for GLuc bioluminescence (**b**), eqFP650 fluorescence (**c**), and FLuc bioluminescence (**d**) over the course of treatment with AMD3100 or vehicle. Filled arrow and open arrow denote start and end of treatament with AMD3100. Inset in B shows quantified bioluminescence from binding of chemokine CXCL12-GLuc to intact 231-NGLuc-CXCR4 cells *in vitro* in the presence of increasing concentrations of AMD3100. Black arrow in the inset shows bioluminescence from cells treated with 1.25 μM AMD3100, which is the approximate concentration in serum of treated mice. Data were presented as mean values ± SEM for bioluminescence photon flux normalized to values prior to beginning treatment. *, $P<0.05$, ***, $P<0.005$.